JOURNAL OF BACTERIOLOGY, Aug. 1992, p. 5063–5071
0021-9193/92/155063-09$02.00/0

Vol. 174, No. 15

Sequence Organization and Regulation of the *Bacillus subtilis menBE* Operon

JEFFREY R. DRISCOLL AND HARRY W. TABER*

Department of Microbiology and Immunology, A-68, Albany Medical College, 47 New Scotland Avenue, Albany, New York 12208

Received 18 March 1992/Accepted 3 June 1992

Menaquinone (MK) plays a central role in the respiratory chain of *Bacillus subtilis*. The biosynthesis of MK requires the formation of a naphthoquinone ring via a series of specific reactions branching from the shikimate pathway. "Early" MK-specific reactions catalyze the formation of *o*-succinylbenzoate (OSB) from isochorismate, and "late" reactions convert OSB to dihydroxynaphthoate, by utilizing an OSB-coenzyme A intermediate. We have cloned and sequenced the *B. subtilis menE* and *menB* genes encoding, respectively, OSB-coenzyme A synthase and dihydroxynaphthoate synthase. The MenB open reading frame encodes a potential polypeptide of 261 amino acid residues with a predicted size of 28.5 kDa, while the MenE open reading frame could encode a 24.4-kDa polypeptide of 220 amino acid residues. Probable promoter sequences were identified by high-resolution primer extension assays. Organization of these genes and regulatory regions was found to be *menBp menB menEp menE*. Expression of *menE* was dependent on both *menEp* and *menBp*, indicating an operonlike organization. A region of dyad symmetry capable of forming a stable RNA secondary structure was found between *menB* and *menE*. Culture cycle-dependent expression of *menB* and *menE* was measured by steady-state transcript accumulation. For both genes, maximal accumulation was found to occur within an hour after the end of exponential growth. The *menBp* and *menEp* promoters have sequences compatible with recognition by the major vegetative form of *B. subtilis* RNA polymerase, $E\sigma^A$. Both promoter regions also were found to contain homologies to a sequence motif previously identified in the *menCDp* region and in promoters for several *B. subtilis* tricarboxylic acid cycle genes.

Menaquinone (MK; vitamin K_2) is a lipophilic, nonprotein redox component in the electron transport chain of *Bacillus subtilis* which mediates electron flow between dehydrogenases and cytochromes (5). In addition to its role in respiration, MK is necessary for successful endospore formation and is involved in regulation of cytochrome formation (10, 28). The formation of MK appears to be regulated during growth of *B. subtilis*, with maximal levels being reached within 1 h (T_1) after the end of exponential growth phase in batch culture (T_0), followed by a rapid decline (10). The lack of MK in endospores of *Bacillus cereus* has been correlated with metabolic dormancy (8). Thus, study of the regulation of MK biosynthesis should provide insights into the factors governing modification of *Bacillus* respiratory chains in response to both the nutritional status of the growth medium and the cellular developmental sequence represented by sporulation.

Much of the enzymology of MK biosynthesis has been carried out with *Escherichia coli* (1, 2). However, the pathway in *B. subtilis* appears to be similar if not identical (20, 29). MK is synthesized from a *men*-specific branch of the shikimate pathway, beginning with the isomerization of chorismate to isochorismate. The products of the *menCDF* genes are necessary for the conversion of isochorismate to *o*-succinylbenzoate (OSB), a stable intermediate in the MK biosynthetic pathway. The conversion of OSB to dihydroxynaphthoate via an OSB-coenzyme A (CoA) intermediate requires the products of *menE* (OSB-CoA synthase) and *menB* (dihydroxynaphthoate synthase). Several MK-deficient strains of *B. subtilis* (29) have been characterized in vitro (20) as to the particular enzymatic function that is deficient. This has permitted cloning of *men*-specific sequences and assignment of gene functions to specific segments of DNA.

The cloning of *menCDBE* has been previously reported, along with preliminary analysis of a promoter (*menCDp*) (13, 21, 22). In subsequent experiments, we discovered that the previously cloned material was unable to rescue the *menE310* mutation (11). This indicated that only a portion of *menE* had been cloned. Genetic disruption studies with integrative plasmid vectors carrying *men*-specific inserts suggested the existence of at least one other transcriptional unit in the *men* cluster. In this study, we undertook cloning the remainder of *menE* and characterization of the transcriptional regulation of *menB* and *menE*.

Here, we report cloning of the 3′ terminus of *menE*, the DNA sequences of *menB* and *menE*, and the relative transcript abundance of both *menB* and *menE* during growth and sporulation; we also identify probable promoters for *menB* and *menE* by transcript mapping.

MATERIALS AND METHODS

Bacterial strains and media. *B. subtilis*, *E. coli*, and bacteriophage strains are listed in Table 1. Growth supplements and antibiotics were from Sigma Chemical Company, and media were from Difco Laboratories. *B. subtilis men* strains were maintained on tryptose blood agar base agar plates containing 0.5% glucose, 18 μM menadione, and 1.5% agar (TG_{18} medium) as previously described (22). *B. subtilis* strains containing integrative plasmids conferring resistance to chloramphenicol were grown on TG_{18} or Luria-Bertani (LB) agar plates containing 5 μg of chloramphenicol (TG_{18}- or LB-C_5) per ml. For RNA isolations, *B. subtilis* strains were grown in 2× Schaeffer's nutrient sporulation medium

* Corresponding author.

TABLE 1. Strains, bacteriophage, and plasmids

Strain, bacteriophage, or plasmid	Relevant characteristics	Source or reference
B. subtilis		
RB1	*trpC2*	This laboratory
RB394	*trpC2 menE310*	This laboratory (29)
RB413	*trpC2 menB325*	This laboratory (29)
RB415	*trpC2 menB329*	This laboratory (29)
E. coli		
JM107	Δ(*lac-proAB*), *thi-1 gyrA96 endA1 hsdR17 relA1 supE44 mcrA* [F′ *traD36 proA lacI*^{q} Δ(*lacZ*)M15]	M. Belfort
ER1451	JM107 *mcrBC*	New England Biolabs
KE89	MM294 *zad*::Tn*10 pcnB80* Tc^r	P. Youngman
Bacteriophage R408	Replication-defective M13 helper	Stratagene
Plasmids		
pSGMU2	Amp^r Cm^r *E. coli* replicon	J. Errington
pBS +/−	Amp^r f1 origin *E. coli* replicon	Stratagene
pKS +/−	Amp^r f1 origin *E. coli* replicon	Stratagene

(22, 26). *E. coli* strains containing plasmid vectors conferring ampicillin resistance were maintained on Luria broth and LB agar plates supplemented with 50 μg of ampicillin per ml or on M9 plates (19) containing 30 μg of ampicillin per ml.

Genetic techniques. *B. subtilis* was transformed by the method of Piggot et al. (24). *E. coli* was transformed by the method of Hanahan (12). Single-stranded DNA was isolated from F$^+$ *E. coli* strains carrying M13-derived plasmids with helper phage R408 by following a standard protocol (4).

In vitro DNA manipulations. Restriction digestions, ligations, and subclonings were performed by following standard protocols (19). All enzymes were from U.S. Biochemical Corp. unless otherwise listed. Chromosomal DNA was isolated from *B. subtilis* strains as described by Saunders et al. (25).

DNA sequencing. Single- and double-stranded DNA was sequenced by the Sanger dideoxy chain termination method by using a modified T7 DNA polymerase (Sequenase) and α-^{35}S-dATP (>1,000 Ci/mmol; Amersham) according to the supplier's protocols. Sequencing reaction products were resolved on 5% acrylamide (20:1 acrylamide/bisacrylamide)–7 M urea gels (National Diagnostics). Dried gels were exposed to X-ray film (X-Omat AR; Kodak) at room temperature for 12 to 72 h. The complete sequence from both strands was determined.

RNase protection assays. Ribonuclease protection assays were performed with an RNase protection assay kit (Ambion, Inc.) by following the manufacturer's standard protocol. Radiolabelled cRNA probes were generated from linearized plasmid clones by utilizing a T7/T3 in vitro transcription kit (Ambion, Inc.) and [α-^{32}P]UTP (>400 Ci/mmol; Amersham). RNA was isolated at specific time points from *B. subtilis* RB1 grown in 2× Schaeffer's sporulation medium as described by Miller et al. (21) and resuspended in diethyl pyrocarbonate-treated distilled water. Protected hybrids were separated by electrophoresis on 5% polyacrylamide–7 M urea sequencing gels. Autoradiography was carried out on the dried gels with intensifying screens at −70°C overnight. The amount of radioactivity in each protected band was quantified directly from the dried gels with a Beta Scope Model 603 Blot Analyzer (Betagen Corporation). Molar ratios were determined from the amount of radioactivity in each protected band and the estimated size of the band.

Primer extension analysis. Synthetic oligonucleotides JD11 (5′-GTCGTCTCTTGCGTCAGC-3′) and JD12 (5′-CAAGC TGTTCCGCCATTCG-3′) (Oligos Etc.) were 5′ end labelled with [γ-^{32}P]ATP (3,000 Ci/mmol; Dupont-New England Nuclear) and T4 polynucleotide kinase by following the supplier's protocol. Oligonucleotides were separated from precursor ATP on Bio-Spin 6 chromatography columns (Bio-Rad).

RNA from *B. subtilis* RB1 or *Saccharomyces cerevisiae* was coprecipitated (19) with radiolabelled oligonucleotide and resuspended in 30 μl of hybridization buffer [80% deionized formamide, 40 mM piperazine-*N*,*N*′-bis(2-ethanesulfonic acid) (pH 6.4), 400 mM sodium acetate (pH 6.4), 1 mM EDTA]. Samples were heated to 85°C for 10 min, incubated at 42°C for 17 to 20 h, and precipitated as described above. The precipitate was resuspended in 21 μl of distilled water. The extension reaction was performed with a first-strand cDNA synthesis kit (Pharmacia LKB) by following the supplier's recommended protocol, except the incubation at 37°C was increased to 2 h. Following the reaction, 0.5 μl of 0.5 M EDTA (pH 8.0) and 1.0 μl of 10 mg of RNase A (Sigma Chemical Co.) per ml were added for 1 h at 37°C. The total volume of the reaction mixture was brought to 100 μl with STE buffer (10 mM Tris-Cl [pH 7.5], 1 mM EDTA, 150 mM NaCl) and extracted with an equal volume of phenol-chloroform-isoamyl alcohol (25:24:1). Aqueous layers were placed on Bio-Spin 6 chromatography columns, and the eluate was precipitated with 2.5 volumes of 100% ethanol. The precipitate was resuspended in 3 μl of distilled water and 2 μl of loading buffer (80% formamide, 0.1% bromophenol blue, 0.1% xylene cyanol, 2 mM EDTA). Primer extension products were resolved on 5% polyacrylamide–7 M urea sequencing gels. Size markers were created by carrying out DNA sequencing reactions with appropriate plasmid subclone templates by using oligonucleotide primers JD11 and JD12.

Nucleotide sequence accession number. The DNA sequence reported here has been deposited with GenBank under accession number M74183.

RESULTS

Cloning of the *menB-menE* region. A previous report described the cloning of DNA sequences from *B. subtilis* capable of rescuing characterized *menB* and *menE* mutations (22). The inability of this cloned material, however, to rescue the *menE310* allele (11) suggested that additional *men* gene cluster sequences needed to be isolated 3′ to those contained

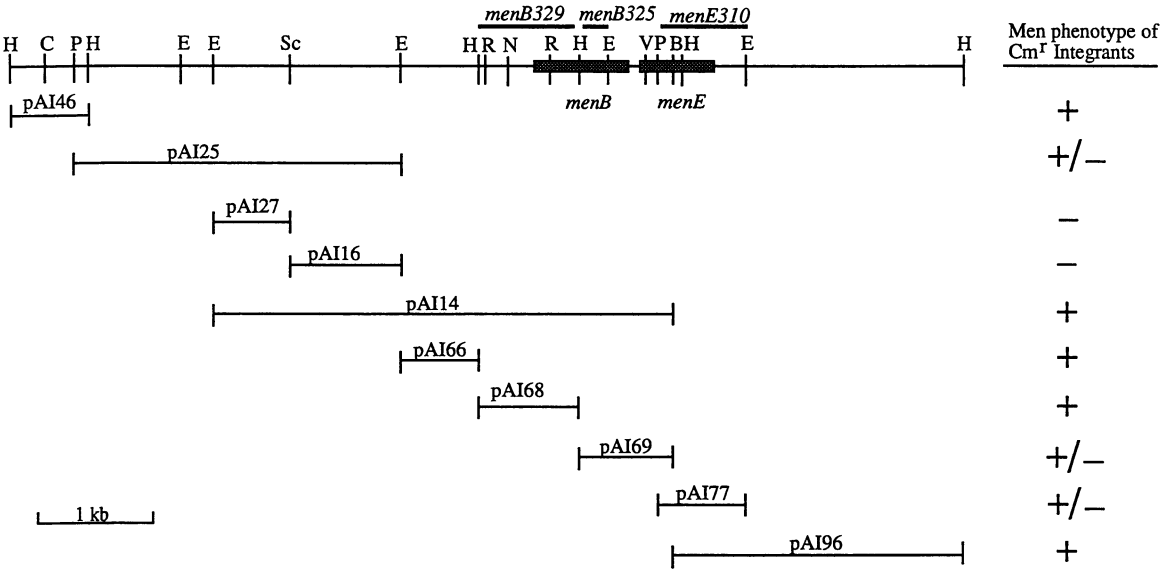

FIG. 1. Genetic and physical map of the *men* locus. Only the *B. subtilis* sequences of the pSGMU2-based vectors are shown (22). These vectors were used to transform strain RB1 to chloramphenicol resistance on TG_{18}-C_5 medium. Cm^r transformants were then screened for Men phenotype on LB-C_5 medium. Abbreviations for restriction sites: B, *Bam*HI; C, *Cla*I; E, *Eco*RI; H, *Hin*dIII; N, *Nla*IV; P, *Pst*I; R, *Rsa*I; Sc, *Sac*I; V, *Pvu*II.

in the integrative plasmid construct pAI14 (Fig. 1). This plasmid was subcloned to yield pAI69. The *Pst*I-*Bam*HI fragment of pAI69 was further subcloned into pSGMU2, and the latter construct was integrated by homologous recombination into the chromosome of strain RB1. Following digestion of integrant chromosomal DNA with *Eco*RI, the outclone pAI77 (Fig. 1) was recovered. The structure of this newly cloned chromosomal DNA was confirmed by Southern blot analysis, and the sequence was found to rescue the *menE310* allele. Integration by homologous recombination of pAI77 into the *B. subtilis* chromosome yielded a $Men^{+/-}$ phenotype. This indicated that the 3′ end of the transcriptional unit encoding *menB* and *menE* was not contained in pAI77. Further outcloning to obtain sequences 3′ to the *Pst*I-*Eco*RI fragment of pAI77 was hampered by the tendency for these sequences to rearrange in *E. coli*. This problem was overcome by utilizing as a cloning host *E. coli* KE89 carrying a *pcnB* mutation which results in a lowered plasmid copy number for ColE1-like plasmids (18). By using this host, several stable outclones representing over approximately 4 kbp of additional material were isolated. All of these outclones (pAI96; Fig. 1) yielded Men^+ integrants when integrated, and they served to rescue the *menE310* mutation. However, subclones derived from these plasmids retained the tendency to rearrange at high frequency in *E. coli* hosts (6).

Genetic analysis of the *menB-menE* region. Having isolated sequences that appeared to represent the remainder of the *men* gene cluster, we constructed subclones for use in marker rescue and genetic disruption experiments. The results are summarized in Fig. 1. The rescue of *menB* alleles by fragments from the 5′ portion of the *menBE* region and the rescue of the *menE310* allele by the *Pst*I-*Eco*RI fragment from the 3′ portion suggested that the order of the two genes is 5′-*menB menE*-3′. The Men phenotype of Cm^r integrants throughout the *men* gene cluster also is summarized in Fig. 1, including data previously reported (22). Whereas pAI27 and pAI16 disrupt the *menCD* transcriptional unit (22), pAI66 does not. This suggests that a transcriptional boundary occurs within pAI66. The 5′ boundary of the transcriptional unit that includes *menB* appears to occur within pAI68, because the chromosomal fragment in this integrative plasmid rescues several *menB* mutations, and does not result in disruption of *men* transcription sufficient to cause a Men^- phenotype (Fig. 1).

The integrative plasmids pAI69 and pAI77 gave anomalous results in the genetic disruption tests (Fig. 1). Rather than clear Men^+ or Men^- phenotypes, Cm^r integrants formed with these plasmids had intermediate growth phenotypes, forming small colonies on unsupplemented LB medium. This property was reminiscent of the previous result obtained with plasmid pAI25 (Fig. 1) integrated into the *menCD* region of the gene cluster (22) and suggests that transcription in both the *menBE* and *menCD* regions has complexities that may involve multiple transcription initiation and termination sites.

Sequence of the *menB-menE* region. DNA sequence analysis revealed two open reading frames (ORFs) (Fig. 2). An ORF apparently corresponding to MenB encodes a potential polypeptide of 261 amino acid residues, with a predicted size of 28.5 kDa; the MenE ORF encodes a potential polypeptide 220 amino acid residues long with a predicted size of 24.4 kDa. The *menE310* allele was cloned and sequenced and found to be a frameshift mutation caused by a cytosine insertion after base 1679, within the MenE ORF. Kyte and Doolittle hydropathy profiles (17) of the predicted polypeptides showed no evidence of possible transmembrane domains, suggesting that MenB and MenE function in the cytoplasm of *B. subtilis* (data not shown). The MenB ORF was found to be highly homologous to *E. coli* MenB (14) and to another CoA-utilizing enzyme, rat enoyl CoA hydratase (23) (Fig. 3). The sequence for MenE from *E. coli* is as yet unavailable (14). The $Men^{+/-}$ phenotype of the pAI69 and pAI77 integrants (Fig. 1) suggested that *menE* possesses a separate promoter (*menEp*) but in addition is dependent on transcription activity from the promoter for *menB* (*menBp*).

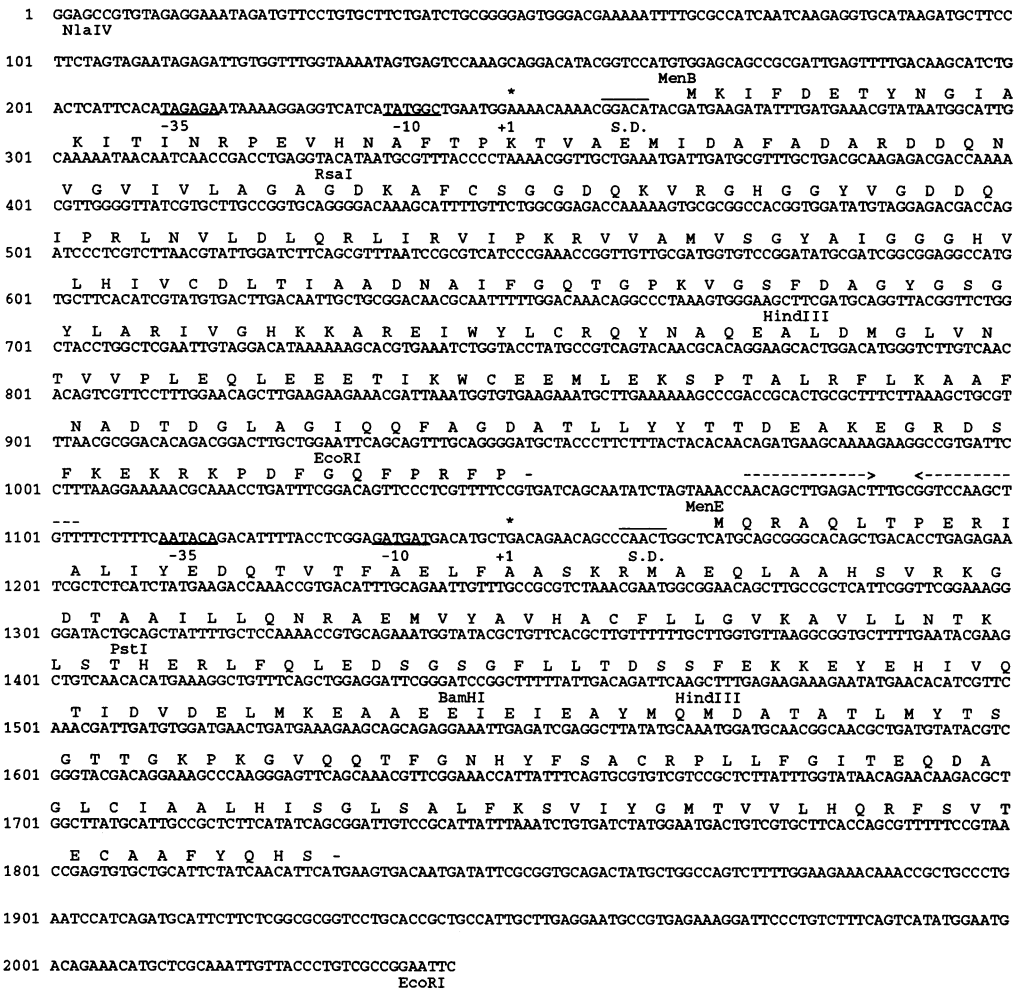

FIG. 2. Sequence of the *menBE* operon. Abbreviations and symbols: S.D., Shine-Dalgarno sequence; *, nucleotides to which RNA 5′ termini map; ———> <———, sequence of dyad symmetry; hyphens, termination codons. Underlined nucleotides indicate probable promoter sequences.

Several potential promoter sequences were found in the region 5′ to the MenB ORF and within the intercistronic region between the MenB and MenE ORFs. These were similar in sequence to other promoters capable of being recognized by the major vegetative form of RNA polymerase in *B. subtilis*, Eσ^A.

The intercistronic region between *menB* and *menE* contains a sequence of dyad symmetry capable of forming an RNA secondary structure with a predicted $\Delta G = -17.9$ (30). Additionally, the loop region within this structure bears homology (5′-CUUUGCGG-3′) to a sequence in the *purFM* intercistronic region of the *pur* operon of *B. subtilis* (5′-CUUUUAGCGG-3′) (7) and to *E. coli* phage T4 terminators (5′-CUUCGG-3′) (31). In the latter situation, this type of loop has been demonstrated to provide thermodynamic stability to RNA secondary structures (31). This structure is predicted to function in rho-independent termination in vivo, on the basis of stability and sequence criteria common to rho-independent terminators in *E. coli* (3).

Characteristics of *menB* and *menE* transcription. The genetic and DNA sequence analyses described above pointed to the likelihood of multiple transcription initiation sites in the *menB-menE* region. Further, they suggested the possibility that genes in separate regions of the *men* locus are regulated differently from one another. This could provide a system for control of MK formation. Previous work on *menCDp* included measurement of transcript accumulation during growth and sporulation (21). To map the approximate 5′ termini of *menB* and *menE* transcripts and to compare the timing of expression from *menB* and *menE* promoters to that from *menCDp*, RNase protection assays were performed. Radiolabelled cRNA probes to the 5′ portion of *menB* were generated by in vitro transcription with T3 RNA polymerase by utilizing as template a plasmid subclone containing the *Rsa*I fragment of pAI68 (Fig. 1). The probe was hybridized in excess to equal amounts of total RNA isolated from culture samples taken at several times during growth and sporulation. In addition to determination of kinetics of transcript accumulation, size estimation of RNase-protected fragments was used to map with low resolution the 5′ terminus of *menB* transcripts. As shown in Fig. 4, the level of *menB* mRNA accumulation began to increase late in vegetative growth (T_v), peaking at T_1, i.e., 1 h after T_0 (the end of exponential growth phase). A rapid decline in *menB* transcript levels began at T_2 and continued through T_4. The kinetics were similar to those found for *menCDp*-induced

FIG. 3. Protein sequence homologies of MenB, based on the DNA sequence of the *menB* gene. Shown is a sequence homology comparison of MenB of *B. subtilis* (bsMenB), MenB of *E. coli* (14) (ecMenB), and rat enoyl-CoA hydratase (23) (enoyl-CoA). ORFs were compared for homology by using the program CDGENE (Hitachi America Ltd.). Colons indicate identical residues; periods indicate similar residues. Broken arrow indicates further sequence not shown.

transcripts (21) and to the kinetics of MK accumulation during batch culture growth (10). Read-through transcription originating upstream from *menBp* also was detected, represented by a high-molecular-weight fragment corresponding to complete protection of *men*-specific sequences in the cRNA probe corresponding to a size of approximately 400 nucleotides (nt) (Fig. 4). Maximum accumulation of read-through transcripts occurred at T_0 through T_1. At T_1, read-through transcripts into *menB* appeared to be present at approximately one-half the molar amount of *menBp*-initiated transcripts.

To examine the possibility that *menE* was transcribed by a promoter separate from *menBp* and to examine the possible role of the *menBE* intercistronic dyad symmetry as a transcriptional terminator, a radiolabelled cRNA probe to the *menBE* intercistronic region was generated from a plasmid subclone containing the *Eco*RI-*Pst*I fragment of pAI69 (Fig. 1) by in vitro transcription with T7 RNA polymerase. Figure 5 shows that a 5′ terminus could be mapped with low resolution to the *menB-menE* intercistronic region, suggesting either that transcription initiates in this region or that processing of *menBp* transcripts occurs between *menB* and *menE*. A cRNA probe to the *Pvu*II-*Pst*I fragment of pAI69 (Fig. 1) was used to confirm that the protected band corresponded to a 5′ terminus for *menE* and not a 3′ terminus for *menB* transcripts (6). The timing of expression of *menEp*-specific transcripts is qualitatively similar to that for *menBp*-initiated transcripts and to those initiated at *menCDp* (21). The *menEp* transcripts are present in a threefold molar excess over *menB* RNA at T_1 (Fig. 5). The levels of read-through transcripts into *menE*, as for read-through into *menB*, peak at T_0 through T_1; the peak is followed by a rapid decline of detectable message at T_2 through T_4. Read-through transcription into *menE* was detected as a protected fragment with a size of approximately 380 nt, corresponding to complete protection from RNase of the *men*-specific sequences in the probe (Fig. 5). The level of read-through into *menE* was approximately 10% of the amount for *menEp*-initiated transcripts at T_1. The smaller protected band in Fig. 5 is the appropriate size for a *menB* transcript terminating at the intercistronic sequence of dyad symmetry. This suggests that the dyad symmetry functions in vivo as a rho-independent terminator.

High-resolution mapping of 5′ termini in the *menBE* operon. The approximate locations of the 5′ termini of *menB* and *menE* messages were determined by RNase protection assays as described above. These termini were then mapped with high resolution by primer extension experiments. In Fig. 6, oligonucleotide JD11 was used to map the 5′ terminus of the *menB* message to an adenine residue at nt 248. The location of this 5′ end suggests that the probable promoter is the sequence located starting at nt 212, 5′-TAGATA-(N_{17})-TATGGC-3′. The sequence suggests that the *menBp* promoter is capable of recognition by the major vegetative form of RNA polymerase in *B. subtilis*, $E\sigma^A$. No other sequence homologies were found for other known recognition signals by sigma factors. The sequence beginning at nt 199, 5′-TGACTCATTCACATA-3′, which overlaps with the probable −35 sequence, is very similar to that found in the *menCDp* region (21) and among several *B. subtilis* promoters for genes involved in the tricarboxylic acid cycle and electron transport (27) (Fig. 8).

Primer extension analysis with oligonucleotide JD12 mapped a *menE* 5′ terminus to the guanosine residue at nt 1148 (Fig. 7). This 5′ terminus suggests that the probable promoter sequence, starting at nt 1112, is 5′-AATACA-(N_{16})-GATGAT-3′. Like *menBp*, *menEp* appears to be recognized by $E\sigma^A$ only. The lower-molecular-weight band corresponds to an adenine residue at nt 1153 and may be due to degradation or processing. A sequence in the *menEp* region beginning at nt 1096, 5′-AAGCTGTTTTCTTTT CAATACAGACATT-3′, which overlaps both the dyad symmetry and the *menEp* −35 region, has a higher degree of similarity than that found in *menBp* with the sequence motif described above. The higher-molecular-weight band, which does not appear in RNase protection assays of the same samples, apparently is an artifact created by pausing of

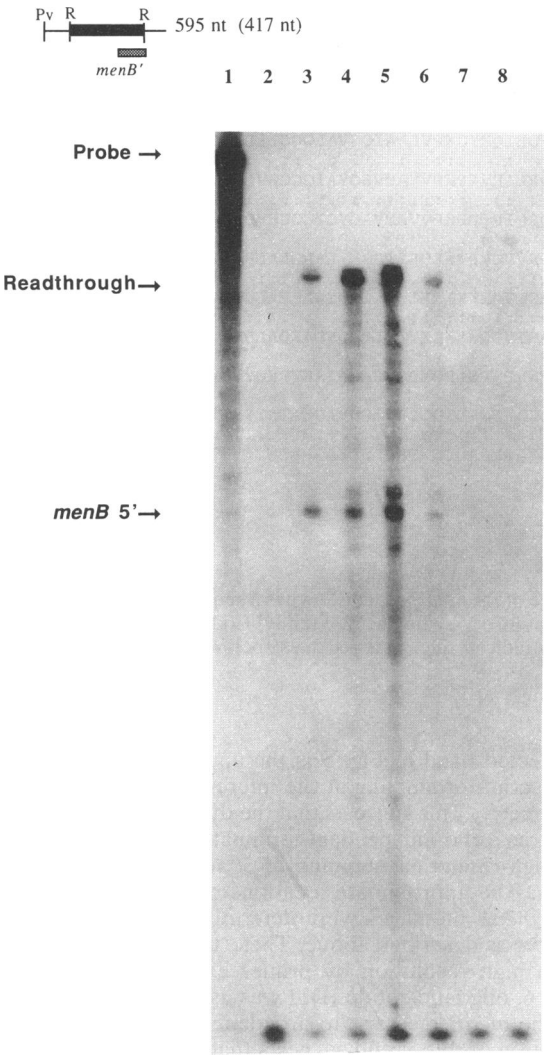

FIG. 4. Accumulation of *menBp*-initiated transcripts during growth and sporulation of strain RB1. RNase protection assays were performed with a 595-nt ^{32}P-labelled antisense cRNA probe. The structure of this probe is shown; it comprised 417 nt of *B. subtilis* chromosomal sequences and 178 nt of pBS sequences and spanned the 5′ end of the *menB* coding region. The probe (4×10^4 cpm) was hybridized with the RNAs indicated and then digested with a combination of RNases A and T_1. Protected hybrids were separated by electrophoresis on 5% polyacrylamide gels containing 7 M urea. An autoradiograph of the dried gel is shown. Bands corresponding to protection of the probe by read-through transcripts and *menBp*-initiated RNAs are indicated by arrows. Lane 1, 4×10^4 cpm probe and 10 μg of yeast RNA not treated with RNase. Lanes 2 to 8, 4×10^4 cpm of probe and indicated RNA digested with RNases A and T_1. Lanes: 2, 10 μg of yeast RNA; 3, 5 μg of total *B. subtilis* RNA isolated from cells during vegetative growth; 4 to 8, 5 μg of total *B. subtilis* RNA isolated from cells at T_0, T_1, T_2, T_3, and T_4, respectively. Restriction sites: Pv, *Pvu*II; R, *Rsa*I.

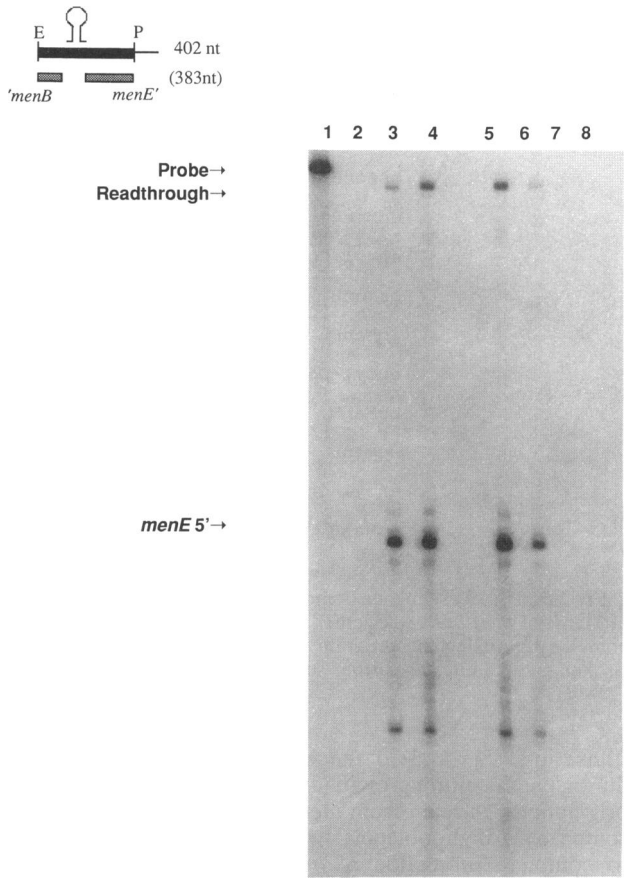

FIG. 5. Accumulation of *menEp*-initiated transcripts during growth and sporulation of strain RB1. RNase protection assays were performed with a 402-nt ^{32}P-labelled antisense cRNA probe. The structure of this probe is shown; it comprised 383 nt of *B. subtilis* chromosomal sequences and 19 nt of pBS sequences and spanned the 5′ end of the *menE* coding region. The probe (7×10^4 cpm) was hybridized with the RNAs indicated and then digested with a combination of RNases A and T_1. Protected hybrids were separated by electrophoresis on 5% polyacrylamide gels containing 7 M urea. An autoradiograph of the dried gel is shown. Bands corresponding to protection of the probe by read-through transcripts and *menEp*-initiated RNAs are indicated by arrows. Lane 1, 7×10^4 cpm of probe and 10 μg of yeast RNA not treated with RNase. Lanes 2 to 8, 7×10^4 cpm of probe and indicated RNA digested with RNases A and T_1. Lanes: 2, 10 μg of yeast RNA; 3; 5 μg of total *B. subtilis* RNA isolated from cells during vegetative growth; 4 to 8; 5 μg of total *B. subtilis* RNA isolated from cells at T_0, T_1, T_2, T_3, and T_4, respectively. Restriction sites: E, *Eco*RI; P, *Pst*I.

reverse transcriptase at the cytosine residue at nt 1085, corresponding to the loop region of the intercistronic dyad symmetry structure.

DISCUSSION

In this article, we describe the cloning, genetic organization, and transcriptional regulation of the *menB* and *menE* genes from *B. subtilis*. Previously, the *men* gene cluster of *B. subtilis* was thought to be transcribed from a single $E\sigma^A$-type promoter, *menCDp* (22). Disruption genetic experiments demonstrated the existence of additional transcriptional units. Cloned *B. subtilis* DNA capable of rescuing biochemically defined *menB* and *menE* mutations was sequenced, and specific functions were assigned to ORFs.

The *menB* and *menE* promoters have been identified by DNA sequencing and high-resolution primer extension mapping. Transcription of *menB* is initiated from an $E\sigma^A$-dependent promoter approximately 19 nt upstream from the probable initiation codon for the *menB* ORF. Transcription from upstream sequences into *menB* accounts for approximately one-half of the *menB* messages at T_1. A sequence of

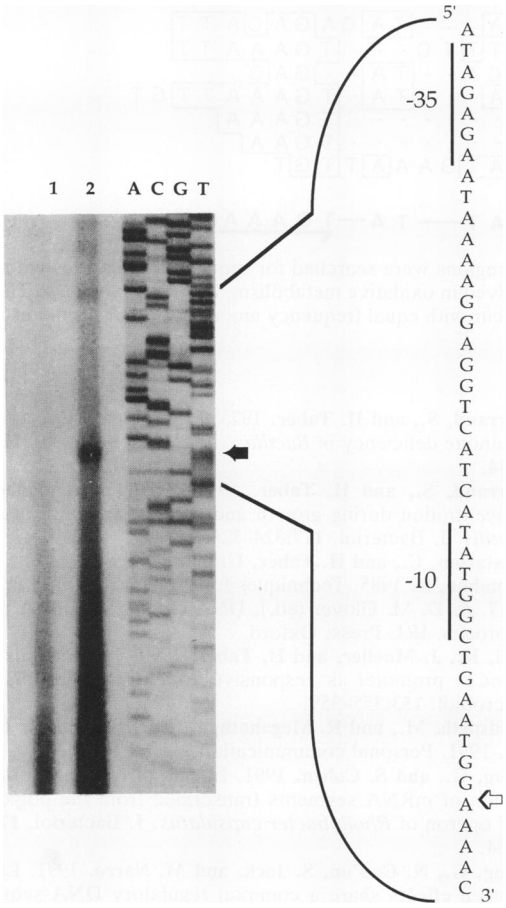

FIG. 6. High-resolution mapping of the *menBp*-initiated transcriptional start site by primer extension. Lanes: 1, 2×10^4 cpm of ^{32}P-end-labelled oligonucleotide (approximately 45 ng) JD11 and 10 μg of yeast RNA treated with reverse transcriptase; 2, extension product obtained by hybridizing JD11 with 5 μg of total *B. subtilis* RNA isolated from cells at T_1 and treated with reverse transcriptase; A, C, G, and T, nucleotide sequence derived from pAI68 by using JD11 as the primer. The solid arrow indicates the sequence fragment corresponding to the extension product. The DNA sequence of the sense strand is shown to indicate the transcription start point (open arrow) and the −35 and −10 regions of *menBp*.

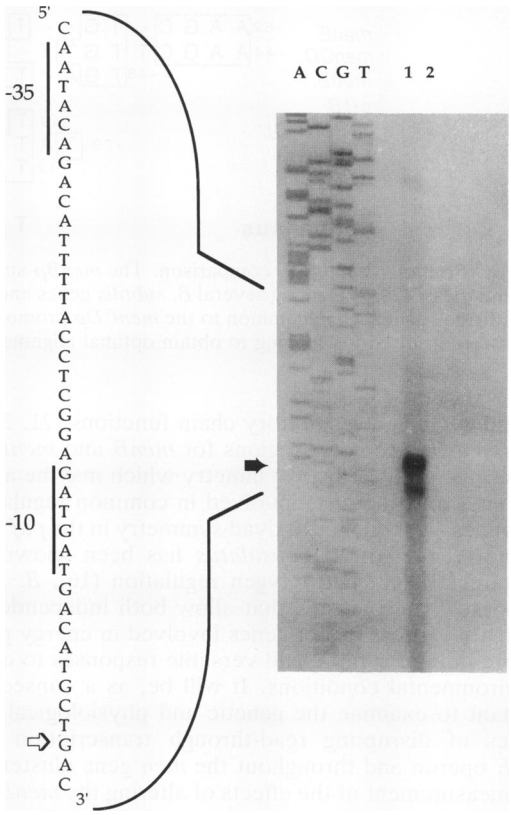

FIG. 7. High-resolution mapping of the *menEp*-initiated transcriptional start site by primer extension. Lanes: 1, extension product obtained by hybridizing 2×10^4 cpm of ^{32}P-end-labelled oligonucleotide (approximately 45 ng) JD12 with 5 μg of total *B. subtilis* RNA isolated from cells at T_1 and treated with reverse transcriptase; 2, 2×10^4 cpm of JD12 and 10 μg of yeast RNA treated with reverse transcriptase; A, C, G, and T, nucleotide sequence derived from pAI69 by using JD12 as the primer. The solid arrow indicates the sequence fragment corresponding to the extension product. The DNA sequence of the sense strand is shown to indicate the transcription start point (open arrow) and the −35 and −10 regions of *menEp*.

dyad symmetry in the intercistronic region between *menB* and *menE* capable of pausing T7 RNA polymerase in vitro (6) apparently functions as a rho-independent terminator. Transcription beyond this putative stem-loop structure continues through *menE*. In addition to read-through transcription, *menE* messages can be formed by initiation at an $E\sigma^A$-dependent promoter approximately 22 nt upstream from the *menE* ORF. The kinetics of expression from *menBp* and *menEp* were examined during growth and sporulation by RNase protection assays. Both *menB* and *menE* messages accumulate to maximal levels within an hour after the end of exponential growth in batch culture. These kinetics are very similar to those previously described (21) for another promoter in the *men* gene cluster, *menCDp*.

The reasons for such complex transcriptional regulation in the *men* gene locus are unknown. Another prokaryotic system which exhibits complex regulation of genes involved in energy production is *Rhodobacter capsulatus* (15, 32). In *R. capsulatus*, there is overlapping transcription of the *crtEF*, *bchCA*, and *puf* operons, which encode products necessary for formation of the photosynthetic apparatus, and there is evidence that the three operons can be expressed as a single transcript (32). Additionally, differential stability of *puf* operon messages has been associated with the progress of translation along certain segments (15).

In *E. coli*, a transcribed uridine-rich sequence in a dyad symmetry located upstream from the initiation codon for *rpoD* has been shown to enhance translation (33). A similar situation could be occurring for *menE* by the *menB-menE* intercistronic dyad symmetry. Although read-through transcription accounts for approximately 10% of *menE* RNA at the time of maximal expression (Fig. 5), the $Men^{+/-}$ phenotype of the pAI69 integrant (Fig. 1) suggests that less than 10% of normal MK levels are being synthesized (9). If the sequence of dyad symmetry enhances the translation of *menE* RNA, it would be, to our knowledge, the first report of that particular regulatory mechanism occurring in a gram-positive organism.

A promoter region sequence homology previously described for *menCDp* and several genes encoding tricarbox-

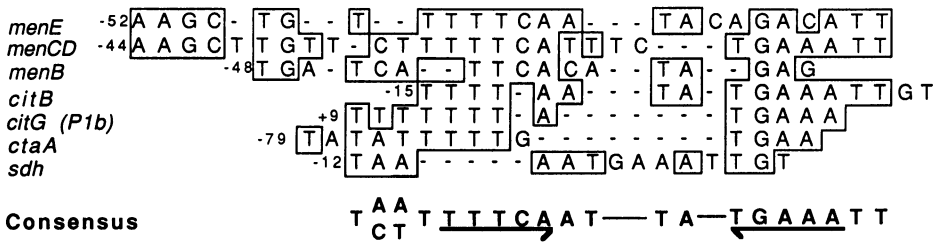

FIG. 8. Promoter homology comparison. The *menBp* and *menEp* promoter regions were searched for sequence similarities with a motif noted previously (21, 27) among several *B. subtilis* genes encoding proteins involved in oxidative metabolism, including *menCDp*. The boxed areas indicate sequences in common to the *menCDp* promoter region or that occur with equal frequency among the other promoter regions. Dashes were inserted for spacing to obtain optimal alignment.

ylic acid cycle and respiratory chain functions (21, 27) also appears in the promoter regions for *menB* and *menE*. This sequence contains a dyad symmetry which may be a recognition site for a factor(s) involved in common regulation of these genes. A sequence of dyad symmetry in the *puf* operon promoter region of *R. capsulatus* has been shown to be important for light and oxygen regulation (16). *B. subtilis* may possess mechanisms that allow both independent and coordinate expressions of genes involved in energy production, providing for rapid and versatile responses to changes in environmental conditions. It will be, as a consequence, important to examine the genetic and physiological consequences of disrupting read-through transcription in the *menBE* operon and throughout the *men* gene cluster. Similarly, measurement of the effects of altering the *menB-menE* intercistronic stem-loop sequence and the *men* promoter sequence homology will begin to provide insights into the mechanisms by which environmental stimuli affect respiratory chain gene expression in *B. subtilis*.

ACKNOWLEDGMENTS

We thank M. Belfort, P. Youngman, J. Errington, and L. Flaherty for strains and plasmids; A. Arrow for oligonucleotides; C. Gustafson for technical assistance; M. Belfort for use of the Beta Scope Blot Analyzer; and J. Mueller for helpful discussion.

REFERENCES

1. **Bentley, R., and R. Meganathan.** 1982. Biosynthesis of vitamin K (menaquinone) in bacteria. Microbiol. Rev. **46:**241–280.
2. **Bentley, R., and R. Meganathan.** 1987. Biosynthesis of the isoprenoid quinones ubiquinone and menaquinone, p. 512–520. *In* F. C. Neidhardt, J. L. Ingraham, K. B. Low, B. Magasanik, M. Schaechter, and H. E. Umbarger (ed.), *Escherichia coli* and *Salmonella typhimurium*: cellular and molecular biology. American Society for Microbiology, Washington, D.C.
3. **d'Aubenton-Carafa, Y., E. Brody, and C. Thermes.** 1990. Prediction of rho-independent *Escherichia coli* transcription terminators. J. Mol. Biol. **216:**835–858.
4. **Dente, L., G. Cesareni, and R. Cortese.** 1983. pEMBL: a new family of single stranded plasmids. Nucleic Acids Res. **11:**1645–1655.
5. **de Vrij, W., B. van den Burg, and W. Konings.** 1987. Spectral and potentiometric analysis of cytochromes from *Bacillus subtilis*. Eur. J. Biochem. **166:**589–595.
6. **Driscoll, J., and H. Taber.** Unpublished data.
7. **Ebbole, D. J., and H. Zalkin.** 1987. Cloning and characterization of a 12-gene cluster from *Bacillus subtilis* encoding nine enzymes for *de novo* purine nucleotide synthesis. J. Biol. Chem. **262:**8274–8287.
8. **Escamilla, J. E., B. Baquera, R. Ramírez, A. García-Horsman, and P. del Arenal.** 1988. Role of menaquinone in inactivation and activation of the *Bacillus cereus* forespore respiratory system. J. Bacteriol. **170:**5908–5912.
9. **Farrand, S., and H. Taber.** 1973. Physiological effects of menaquinone deficiency in *Bacillus subtilis*. J. Bacteriol. **115:**1035–1044.
10. **Farrand, S., and H. Taber.** 1974. Changes in menaquinone concentration during growth and early sporulation in *Bacillus subtilis*. J. Bacteriol. **117:**324–326.
11. **Gustafson, C., and H. Taber.** Unpublished data.
12. **Hanahan, D.** 1985. Techniques for transformation of *E. coli*, p. 1–17. *In* D. M. Glover (ed.), DNA cloning, vol. I. A practical approach. IRL Press, Oxford.
13. **Hill, K., J. Mueller, and H. Taber.** 1990. The *Bacillus subtilis menCD* promoter is responsive to extracellular pH. Arch. Microbiol. **153:**355–359.
14. **Hudspeth, M., and R. Meganathan. (Northern Illinois University).** 1991. Personal communication.
15. **Klug, G., and S. Cohen.** 1991. Effects of translation on degradation of mRNA segments transcribed from the polycistronic *puf* operon of *Rhodobacter capsulatus*. J. Bacteriol. **173:**1478–1484.
16. **Klug, G., N. Gad'on, S. Jock, and M. Narro.** 1991. Light and oxygen effects share a common regulatory DNA sequence in *Rhodobacter capsulatus*. Mol. Microbiol. **5:**1235–1239.
17. **Kyte, J., and R. F. Doolittle.** 1982. A simple method for displaying the hydropathic character of a protein. J. Mol. Biol. **157:**105–132.
18. **Liu, J., and J. S. Parkinson.** 1989. Genetics and sequence analysis of the *pcnB* locus, an *Escherichia coli* gene involved in plasmid copy number control. J. Bacteriol. **171:**1254–1261.
19. **Maniatis, T., E. Fritsch, and J. Sambrook.** 1982. Molecular cloning: a laboratory manual. Cold Spring Harbor Laboratory, Cold Spring Harbor, N.Y.
20. **Meganathan, R., R. Bentley, and H. Taber.** 1981. Identification of *Bacillus subtilis men* mutants which lack *o*-succinylbenzoylcoenzymeA synthetase and dihydroxynaphthoate synthase. J. Bacteriol. **148:**328–332.
21. **Miller, P., J. Mueller, K. Hill, and H. Taber.** 1988. Transcriptional regulation of a promoter in the *men* gene cluster of *Bacillus subtilis*. J. Bacteriol. **170:**2742–2748.
22. **Miller, P., A. Rabinowitz, and H. Taber.** 1988. Molecular cloning and preliminary genetic analysis of the *men* gene cluster of *Bacillus subtilis*. J. Bacteriol. **170:**2735–2741.
23. **Minami-Ishii, N., S. Taketani, T. Osumi, and T. Hashimoto.** 1989. Molecular cloning and sequence analysis of the cDNA for rat mitochondrial enoyl-CoA hydratase. Eur. J. Biochem. **185:** 73–78.
24. **Piggot, P. J., C. A. M. Curtis, and H. deLancastre.** 1984. Demonstration of a polycistronic transcription unit required for sporulation of *Bacillus subtilis* by use of integrational plasmid vectors. J. Gen. Microbiol. **130:**2123–2136.
25. **Saunders, C. W., B. J. Schmidt, M. S. Mirot, L. D. Thompson, and M. S. Guyer.** 1984. Use of chromosomal integration in the establishment and expression of *blaZ*, a *Staphylococcus aureus* β-lactamase gene, in *Bacillus subtilis*. J. Bacteriol. **157:**718–726.
26. **Schaeffer, P., J. Millet, and J. Aubert.** 1965. Catabolite repression of bacterial sporulation. Proc. Natl. Acad. Sci. USA **54:**704–711.

27. **Sonenshein, A. L.** 1989. Metabolic regulation of sporulation and other stationary-phase phenomena, p. 109–130. *In* I. Smith, R. A. Slepecky, and P. Setlow (ed.), Regulation of procaryotic development. American Society for Microbiology, Washington, D.C.
28. **Taber, H.** 1980. Functions of vitamin K_2 in microorganisms, p. 177–187. *In* J. W. Suttie (ed.), Vitamin K metabolism and vitamin K-dependent proteins. University Park Press, Baltimore.
29. **Taber, H. W., E. A. Dellers, and L. R. Lombardo.** 1981. Menaquinone biosynthesis in *Bacillus subtilis*: isolation of *men* mutants and evidence for clustering of *men* genes. J. Bacteriol. **145:**321–327.
30. **Tinoco, I., P. N. Borer, B. Dengler, M. D. Levine, O. C. Uhlenbeck, D. M. Crothers, and J. Gralla.** 1973. Improved estimation of secondary structure in ribonucleic acids. Nature (London) New Biol. **246:**40–41.
31. **Tuerk, C., P. Gauss, C. Thermes, D. Groebe, M. Gayle, N. Guild, G. Stormo, Y. d'Aubenton-Carafa, O. Uhlenbeck, I. Tinoco, Jr., E. Brody, and L. Gold.** 1988. CUUCGG hairpins: extraordinarily stable RNA secondary structures associated with various biochemical processes. Proc. Natl. Acad. Sci. USA **85:**1364–1368.
32. **Wellington, C., and J. Beatty.** 1991. Overlapping mRNA transcripts of photosynthesis gene operons in *Rhodobacter capsulatus*. J. Bacteriol. **173:**1432–1443.
33. **Zhang, J., and M. P. Deutscher.** 1992. A uridine-rich sequence required for translation of prokaryotic mRNA. Proc. Natl. Acad. Sci. USA **89:**2605–2609.